Int. J. Heat Mass Transfer. Vol. 26, No. 8, pp. 1143–1149, 1983
Printed in Great Britain

0017-9310/83 $3.00+0.00

CERTAIN HEAT TRANSFER PROBLEMS IN A RECTANGULAR REGION WITH MULTIPLE CUTOUTS

A. K. NAGHDI

Purdue University School of Engineering and Technology and School of Science at Indianapolis, IA 46223, U.S.A.

(*Received* 7 *July* 1982 *and in final form* 9 *December* 1982)

Abstract—Employing a new class of functions, obtained from the refinement of a previous technique, the following steady-state heat transfer problems are solved: (1) A prismatic rectangular bar is cooled or heated by a fluid flowing in the circular cutouts of the bar. (2) Heat transfer in a rectangular region having uniformly distributed heat sources in the circular inserts of different thermal conductivity. (3) Heat conduction in a multiple hole rectangular bar having different inner and outer boundary temperatures. It is assumed that the properties of the materials involved are temperature independent. Numerical results for the cases of rectangular regions with 4 and 8 cavities are presented.

NOMENCLATURE

a,	cross-section length;
A_l,	unknown constants of integration;
$\bar{A}_n$,	unknown constants of integration;
b,	cross-section width;
B_l,	unknown constants of integration;
$\bar{B}_n$,	unknown constants of integration;
c, d, c_1, d_1, c_2, d_2,	coordinates of the centers of the cavities;
$\bar{c}, \bar{d}, \bar{c}_1, \bar{d}_1, \bar{c}_2, \bar{d}_2$,	dimensionless coordinates of the centers of the cavities;
C^*,	axial rate of change of temperature;
C_p,	specific heat at constant pressure;
$f_1, f_2, \bar{f}_1, \bar{f}_2$,	functions defined in equations (9), (11), (13) and (15);
h_{ave},	average convection heat transfer coefficient;
i,	$\sqrt{-1}$;
k_1, k_2,	thermal conductivities of the two materials;
K,	ratio, k_1/k_2;
m,	terms in the series solution;
M,	number of selected points on one of the inner boundaries;
n,	terms in the series solution;
N,	number of holes in each quadrant;
Nu,	Nusselt number;
p,	pressure;
p_1, p_2,	number of terms chosen in the series solution;
P,	axial rate of change of pressure;
q,	uniformly distributed heat source;
Q,	rate of total heat transfer;
r_0,	radius of each cavity;
r,	radius of the path of integration for the Green's function;
$\bar{S}$,	conduction shape factor per unit length;
T_1, T_2,	temperatures respectively in regions 1 and 2;
$\bar{T}_1, \bar{T}_2$,	nondimensional values of T_1, T_2;
$\bar{T}_l^*, \bar{T}_l^0, \bar{T}_l^{(*)}, \bar{T}_l^{(0)}$,	various eigenfunctions in the solution;
T_{1i},	uniform temperature of the inner circles;
$\tilde{T}_c$,	the Green's function for the concentrated source;
T_w,	outside wall temperature;
w, w_0,	velocities of the fluid at a given point and at the centers of the cutouts;
$\bar{w}$,	ratio, w/w_0;
x, y, z,	rectangular coordinates.

Greek symbols

α,	thermal diffusivity;
∇^2,	Laplace operator;
η, η_0,	dimensionless variables, y/a, y_0/a;
φ, φ_0,	polar angles shown in Fig. 1;
ρ,	nondimensional coordinate, r/a;
ρ_0, ρ,	dimensionless values, r_0/a, r/a;
ρ_2^*,	fluid mass density;
λ_1, λ_2,	quantities defined in equations (21) and (26);
$\Lambda_1, \Lambda_2, \Lambda_3, \Lambda_4$,	expressions defined in equations (7);
μ,	dynamic viscosity;
ξ, ξ_0,	dimensionless quantities, x/a, x_0/a.

Subscripts

1, 2,	regions outside, and inside the circular cavities, respectively;
ave,	average;
i,	inner boundary;
w,	wall.

Superscripts

*, 0, (*), (0),	symbols differentiating various eigenfunctions.

INTRODUCTION

IN RECENT years a few authors have investigated problems similar to those solved in this article. Sparrow and Loeffler [1, 2] utilized polar coordinates in order to obtain solutions for a fully developed laminar flow and the related fully developed heat transfer in arrays of tubes arranged in triangular and square forms. Since they assumed an infinitely long and wide cross-sectional area for the arrays, their solutions were reduced to those for the cases of flow and heat transfer around one tube. The continuity condition along each plane separating the regions was then fulfilled through the point-by-point technique. Rowley and Payne [3] employed Howland functions [4] in order to obtain a solution for the problem of a heat generating cylinder cooled by a ring of fluid carrying holes. They assumed a convective boundary condition at the inner holes with a constant convection heat transfer coefficient h. Mathematically, the problems investigated in this article are somewhat more complicated than those solved in refs. [1, 2] as the regions of the boundary value problems are finite. The approximation of h = constant shall not be employed here for case (1). Instead, the exact boundary conditions of equality of temperatures and the rate of heat flows in the solid and fluid at the boundaries of the cutouts are utilized. The mathematical portion of this investigation is based upon the refinement of a technique developed in the author's recent investigation [5]. The basic original functions automatically satisfy a homogeneous outer boundary condition, and have singularity in each quadrant. The poles of these basic functions can be placed at any desired location and they can be repeated, thus, producing sets of functions suitable for $4N$ cutouts symmetrically located with respect to the axes of symmetry of the cross-section. However, in each quadrant the N holes need not be of the same size, nor shall they be located in any orderly fashion. The inner boundary conditions are satisfied through the point-by-point technique and the employment of the method of least square error [6].

The polar coordinate technique used in refs. [1, 2] and the Howland functions method employed in ref. [3] are not suitable for rectangular regions with multiple cutouts. This fact is especially true for the case of a narrow rectangle having more holes along its length than its width.

METHOD OF SOLUTION

In the following, the basic eigenfunctions suitable for a rectangular region with four cutouts (Fig. 1) are derived. Later on, the poles of these singular functions are placed at different points to obtain sets of solutions for a multiple hole region. It is assumed that the portion of the rectangular region outside the holes contains no heat sources, and that its outer boundary is maintained at a constant temperature T_w. The governing differential equation for the temperature T_1 in this region is given by

$$\bar{\nabla}^2\bar{T}_1 = 0, \quad \bar{\nabla}^2 = \partial^2/\partial\xi^2+\partial^2/\partial\eta^2,$$

$$\xi = x/a, \quad \eta = y/a,$$

$$\bar{T}_1 = \frac{T_1-T_w}{T_w} \quad \text{for cases (1) and (2),} \tag{1}$$

$$\bar{T}_1 = \frac{T_1-T_w}{T_{1i}-T_w} \quad (T_{1i} = \text{inner temperature}) \quad \text{for case (3),}$$

subject to the outer boundary condition

$$\bar{T}_1 = 0 \quad \text{at} \begin{cases} \xi = \pm 1/2, \\ \eta = \pm b/(2a). \end{cases} \tag{2}$$

The inner boundary conditions for various cases shall be discussed later. The eigenfunctions of equation (1) automatically satisfying condition (2) were derived in the form of integrals in investigation [5]

$$\begin{aligned} \bar{T}_l^* &= \int_0^{2\pi} \bar{T}_c(\xi,\eta,\xi_0,\eta_0)\cos(l\varphi_0)\bar{\rho}\; d\varphi_0, \\ &\qquad\qquad l = 0,1,2,3,\ldots, \\ \bar{T}_l^o &= \int_0^{2\pi} \bar{T}_c(\xi,\eta,\xi_0,\eta_0)\sin(l\varphi_0)\bar{\rho}\; d\varphi_0, \\ &\qquad\qquad l = 1,2,3,\ldots, \end{aligned} \tag{3}$$

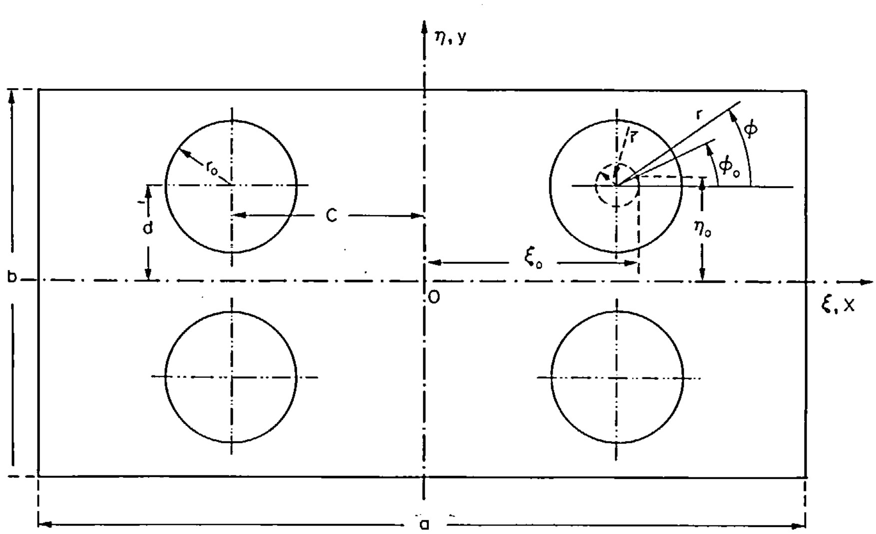

FIG. 1. Rectangular section with four circular cutouts.

in which

$$\tilde{T}_c(\xi,\eta,\xi_0,\eta_0) = \sum_{n=1,3,5}^{\infty} [4/(n\pi)] \times \left\{\frac{\cosh(n\pi\eta_0)\sinh[n\pi(\eta-\frac{1}{2}b/a)]}{\cosh(\frac{1}{2}n\pi b/a)}\right\} \times \cos(n\pi\xi)\cos(n\pi\xi_0) \quad \text{for} \quad b/(2a) \geqslant \eta \geqslant \eta_0,$$

$$\tilde{T}_c(\xi,\eta,\xi_0,\eta_0) = \sum_{n=1,3,5}^{\infty} [4/(n\pi)] \times \left\{\frac{\cosh(n\pi\eta)\sinh[n\pi(\eta_0-\frac{1}{2}b/a)]}{\cosh(\frac{1}{2}n\pi b/a)}\right\} \times \cos(n\pi\xi)\cos(n\pi\xi_0) \quad \text{for} \quad \eta_0 > \eta > -\eta_0, \tag{4}$$

and the integrations are carried over a circular path with a very small but finite radius $\bar{r} = \bar{\rho}a$ (Fig. 1). In investigation [5] the Green's function $\tilde{T}_c$ was obtained by prescribing sets of line sources in the form of Fourier series along $\eta = \pm\eta_0$, and by the limiting process as the segmental line sources tend to point sources.

Unlike the previous investigation [5], the integrations of $\tilde{T}_c$ here are carried out analytically and the limiting functions for $\bar{T}_l^*$ and $\bar{T}_l^0$ are obtained as $\bar{\rho}$ tends to zero. Thus, writing

$$\xi_0 = \bar{c}+\bar{\rho}\cos\varphi_0, \quad \bar{c} = c/a, \qquad \eta_0 = \bar{d}+\bar{\rho}\sin\varphi_0, \quad \bar{d} = d/a, \tag{5}$$

it is found

$$\cosh(n\pi\eta_0)\cos(n\pi\xi_0) = \cos(n\pi\bar{c})\cosh(n\pi\bar{d})\Lambda_1 + \mathrm{i}\cos(n\pi\bar{c})\sinh(n\pi\bar{d})\Lambda_2 - \sin(n\pi\bar{c})\cosh(n\pi\bar{d})\Lambda_3 + \mathrm{i}\sin(n\pi\bar{c})\sinh(n\pi\bar{d})\Lambda_4, \tag{6}$$

in which

$$\begin{aligned}\Lambda_1 &= \cos(n\pi\bar{\rho}\cos\varphi_0)\cos(\mathrm{i}\,n\pi\bar{\rho}\sin\varphi_0),\\ \Lambda_2 &= \cos(n\pi\bar{\rho}\cos\varphi_0)\sin(\mathrm{i}\,n\pi\bar{\rho}\sin\varphi_0),\\ \Lambda_3 &= \sin(n\pi\bar{\rho}\cos\varphi_0)\cos(\mathrm{i}\,n\pi\bar{\rho}\sin\varphi_0),\\ \Lambda_4 &= \sin(n\pi\bar{\rho}\cos\varphi_0)\sin(\mathrm{i}\,n\pi\bar{\rho}\sin\varphi_0),\\ \mathrm{i} &= \sqrt{-1}.\end{aligned} \tag{7}$$

The functions Λ_1–Λ_4 are now expanded into infinite series. Thus, it is found

$$\begin{aligned}\Lambda_1 &= (1/2)\{\cos[n\pi\bar{\rho}(\cos\varphi_0+\mathrm{i}\sin\varphi_0)] + \cos[n\pi\bar{\rho}(\cos\varphi_0-\mathrm{i}\sin\varphi_0)]\}\\ &= (1/2)[\cos(n\pi\bar{\rho}\,\mathrm{e}^{\mathrm{i}\varphi_0})+\cos(n\pi\bar{\rho}\,\mathrm{e}^{-\mathrm{i}\varphi_0})]\\ &= (1/2)\left[1-\frac{(n\pi\bar{\rho}\,\mathrm{e}^{\mathrm{i}\varphi_0})^2}{2!}+\frac{(n\pi\bar{\rho}\,\mathrm{e}^{\mathrm{i}\varphi_0})^4}{4!}-\dots + 1-\frac{(n\pi\bar{\rho}\,\mathrm{e}^{-\mathrm{i}\varphi_0})^2}{2!}+\frac{(n\pi\bar{\rho}\,\mathrm{e}^{-\mathrm{i}\varphi_0})^4}{4!}-\dots\right]\\ &= \sum_{m=0}^{\infty}(-1)^m\frac{(n\pi\bar{\rho})^{2m}}{(2m)!}\cos 2m\varphi_0.\end{aligned} \tag{8}$$

The other functions can be written in Fourier series in the same fashion. The expanded forms of Λ_1–Λ_4 and other similar functions make it possible to carry out the integrations in (3) analytically. For the regions in which $||\eta|-\bar{d}| \geqslant \bar{\rho}$ this procedure leads to the determination of the eigenfunctions in single series forms. However, for the regions $||\eta|-\bar{d}| < \bar{\rho}$ the process does not yield a single series solution for $\bar{T}_l^*$ and $\bar{T}_l^0$ as the two forms of the Green's function given in equation (4) must be employed. In order to eliminate this difficulty, the radius of the path of integration is shrunk to zero. Absorbing the n independent quantities such as

$$\bar{\rho}(-1)^m\frac{(\pi\bar{\rho})^{2m}}{(2m)!}$$

into the unknown coefficients of the eigenfunctions, gives

$$\bar{T}_{2m}^* = (-1)^m \sum_{n=1,3,5}^{\infty} \frac{(n)^{2m-1}\cos(n\pi\bar{c})\cosh(n\pi\bar{d})}{\cosh(\frac{1}{2}n\pi b/a)} f_1(\xi,\eta),$$
$$f_1(\xi,\eta) = \sinh[n\pi(\eta-\tfrac{1}{2}b/a)]\cos(n\pi\xi) \quad \text{for} \quad \tfrac{1}{2}b/a \geqslant \eta > \bar{d}, \quad m = 0,1,2,3,\dots, \tag{9}$$

$$\begin{aligned}\bar{T}_{2m-1}^* &= (-1)^m \sum_{n=1,3,5}^{\infty} \frac{(n)^{2m-2}\sin(n\pi\bar{c})\cosh(n\pi\bar{d})}{\cosh(\frac{1}{2}n\pi b/a)} f_1(\xi,\eta),\\ \bar{T}_{2m}^0 &= (-1)^{m+1} \sum_{n=1,3,5}^{\infty} \frac{(n)^{2m-1}\sin(n\pi\bar{c})\sinh(n\pi\bar{d})}{\cosh(\frac{1}{2}n\pi b/a)} f_1(\xi,\eta),\\ \bar{T}_{2m-1}^0 &= (-1)^m \sum_{n=1,3,5}^{\infty} \frac{(n)^{2m-2}\cos(n\pi\bar{c})\sinh(n\pi\bar{d})}{\cosh(\frac{1}{2}n\pi b/a)} f_1(\xi,\eta),\\ &\text{for} \quad \tfrac{1}{2}b/a \geqslant \eta > \bar{d}, \quad m = 1,2,3,\dots,\end{aligned} \tag{10}$$

$$\bar{T}_{2m}^* = (-1)^m \sum_{n=1,3,5}^{\infty} \frac{(n)^{2m-1}\sinh[n\pi(\bar{d}-\frac{1}{2}b/a)]\cos(n\pi\bar{c})}{\cosh(\frac{1}{2}n\pi b/a)} f_2(\xi,\eta),$$
$$f_2(\xi,\eta) = \cosh(n\pi\eta)\cos(n\pi\xi) \quad \text{for} \quad \bar{d} > \eta > -\bar{d}, \quad m = 0,1,2,3,\dots, \tag{11}$$

$$
\begin{aligned}
\bar{T}^{*}_{2m-1} &= (-1)^m \sum_{n=1,3,5}^{\infty} \frac{(n)^{2m-2}\sinh[n\pi(\bar{d}-\tfrac{1}{2}b/a)]\sin(n\pi\bar{c})}{\cosh(\tfrac{1}{2}n\pi b/a)} f_2(\xi,\eta),\\
\bar{T}^{0}_{2m} &= (-1)^{m+1} \sum_{n=1,3,5}^{\infty} \frac{(n)^{2m-1}\cosh[n\pi(\bar{d}-\tfrac{1}{2}b/a)]\sin(n\pi\bar{c})}{\cosh(\tfrac{1}{2}n\pi b/a)} f_2(\xi,\eta),\\
\bar{T}^{0}_{2m-1} &= (-1)^m \sum_{n=1,3,5}^{\infty} \frac{(n)^{2m-2}\cosh[n\pi(\bar{d}-\tfrac{1}{2}b/a)]\cos(n\pi\bar{c})}{\cosh(\tfrac{1}{2}n\pi b/a)} f_2(\xi,\eta),\\
&\text{for}\quad \bar{d} > \eta > -\bar{d},\quad m = 1,2,3,\ldots.
\end{aligned}
\tag{12}
$$

Similar expressions are written for the region $-\bar{d} > \eta > -(b/2a)$ by the consideration of symmetry. The eigenfunctions so derived have certain disadvantages from the point of view of obtaining numerical results. First of all, the series solutions (9)–(12) are divergent along the lines $\eta = \bar{d}$ and $\eta = -\bar{d}$ for $m > 0$. Secondly, the convergence of these series solutions are poor for small values of $||\eta|-\bar{d}|$. To overcome this difficulty, the following technique is introduced. Consider the cross-section of the rectangular bar if it is rotated $\pi/2$ radians. Employing the same procedure as before, the eigenfunctions with respect to $\bar{\xi} = (a/b)\eta$ and $\bar{\eta} = (a/b)\xi$ are derived. Thus, the sinusoidal terms contain η rather than ξ. For the sake of brevity the intermediate steps are avoided, and only the final results are presented.

$$
\begin{aligned}
\bar{T}^{(*)}_{2m} &= (a/b)^{2m} \sum_{n=1,3,5}^{\infty} \frac{(n)^{2m-1}\cos(n\pi a\bar{d}/b)\cosh(n\pi a\bar{c}/b)}{\cosh(\tfrac{1}{2}n\pi a/b)} \bar{f}_1(\xi,\eta),\\
\bar{f}_1(\xi,\eta) &= \sinh[n\pi a(\xi-\tfrac{1}{2})/b]\cos(n\pi\eta a/b),\quad \text{for}\quad \tfrac{1}{2} > \xi > \bar{c},\quad m = 0,1,2,3,\ldots,
\end{aligned}
\tag{13}
$$

$$
\begin{aligned}
\bar{T}^{(*)}_{2m-1} &= (a/b)^{2m-1} \sum_{n=1,3,5}^{\infty} \frac{(n)^{2m-2}\cos(n\pi a\bar{d}/b)\sinh(n\pi a\bar{c}/b)}{\cosh(\tfrac{1}{2}n\pi a/b)} \bar{f}_1(\xi,\eta),\\
\bar{T}^{(0)}_{2m} &= (a/b)^{2m} \sum_{n=1,3,5}^{\infty} \frac{(n)^{2m-1}\sin(n\pi a\bar{d}/b)\sinh(n\pi a\bar{c}/b)}{\cosh(\tfrac{1}{2}n\pi a/b)} \bar{f}_1(\xi,\eta),\\
\bar{T}^{(0)}_{2m-1} &= (a/b)^{2m-1} \sum_{n=1,3,5}^{\infty} \frac{(n)^{2m-2}\sin(n\pi a\bar{d}/b)\cosh(n\pi a\bar{c}/b)}{\cosh(\tfrac{1}{2}n\pi a/b)} \bar{f}_1(\xi,\eta),\\
&\text{for}\quad \tfrac{1}{2} > \xi > \bar{c},\quad m = 1,2,3,\ldots,
\end{aligned}
\tag{14}
$$

$$
\begin{aligned}
\bar{T}^{(*)}_{2m} &= (a/b)^{2m} \sum_{n=1,3,5}^{\infty} \frac{(n)^{2m-1}\sinh[n\pi a(\bar{c}-\tfrac{1}{2})/b]\cos(n\pi a\bar{d}/b)}{\cosh(\tfrac{1}{2}n\pi a/b)} \bar{f}_2(\xi,\eta),\\
\bar{f}_2(\xi,\eta) &= \cosh(n\pi a\xi/b)\cos(n\pi a\eta/b),\quad m = 0,1,2,3,\ldots,\quad \text{for}\quad \bar{c} > \xi > -\bar{c},
\end{aligned}
\tag{15}
$$

$$
\begin{aligned}
\bar{T}^{(*)}_{2m-1} &= (a/b)^{2m-1} \sum_{n=1,3,5}^{\infty} \frac{(n)^{2m-2}\cosh[n\pi a(\bar{c}-\tfrac{1}{2})/b]\cos(n\pi a\bar{d}/b)}{\cosh(\tfrac{1}{2}n\pi a/b)} \bar{f}_2(\xi,\eta),\\
\bar{T}^{(0)}_{2m} &= (a/b)^{2m} \sum_{n=1,3,5}^{\infty} \frac{(n)^{2m-1}\cosh[n\pi a(\bar{c}-\tfrac{1}{2})/b]\sin(n\pi a\bar{d}/b)}{\cosh(\tfrac{1}{2}n\pi a/b)} \bar{f}_2(\xi,\eta),\\
\bar{T}^{(0)}_{2m-1} &= (a/b)^{2m-1} \sum_{n=1,3,5}^{\infty} \frac{(n)^{2m-2}\sinh[n\pi a(\bar{c}-\tfrac{1}{2})/b]\sin(n\pi a\bar{d}/b)}{\cosh(\tfrac{1}{2}n\pi a/b)} \bar{f}_2(\xi,\eta),\\
&\text{for}\quad \bar{c} > \xi > -\bar{c},\quad m = 1,2,3,\ldots.
\end{aligned}
\tag{16}
$$

Mathematically, the values of the series solutions for $\bar{T}^{*}_{j}$ and $\bar{T}^{0}_{j}$ are identical to those obtained from $\bar{T}^{(*)}_{j}$ and $\bar{T}^{(0)}_{j}$. This fact also has been verified numerically. Therefore, at the points where one of the two sets of series are divergent, or slowly convergent, the other set with rapid convergence properties may be utilized.

The solution for the outer region 1 is now written as

$$
\bar{T}_1 = \sum_{l=0,1,2}^{\infty} A_l \bar{T}^{*}_{l} + \sum_{l=1,2,3}^{\infty} B_l \bar{T}^{0}_{l}, \tag{17}
$$

in which A_l and B_l are the unknown coefficients to be determined.

INNER BOUNDARY CONDITIONS

The eigenfunctions derived in the previous section automatically satisfy the outer boundary condition $\bar{T}_1 = 0$. For cases (1) and (2) the boundary conditions at the inner cutouts are

$$
\begin{aligned}
\bar{T}_1 &= \bar{T}_2,\\
\partial\bar{T}_1/\partial\rho &= (k_2/k_1)\partial\bar{T}_2/\partial\rho,
\end{aligned}
\tag{18}
$$

in which $\bar{T}_2$ is the dimensionless temperature in region 2 (the region inside the cutouts), k_1 and k_2 are respectively the thermal conductivities of the materials in regions 1 and 2, and ρ represents the direction normal to the cutout. For case (3) the inner boundary condition is simply given by

$$\bar{T}_{1i} = 1. \tag{19}$$

FORMULATION OF $\bar{T}_2$ AND NUMERICAL RESULTS

Without the loss of generality, in the following analysis only the cases of bars with four cutouts are discussed. Due to the condition of symmetry it is sufficient to consider the temperature distribution in one of the circular regions. For case (1) of fully developed laminar flow and fully developed heat transfer the governing equations are given by

$$\begin{gathered}\bar{\nabla}^2\bar{w} = (a^2P)/(\mu w_0), \quad \bar{w} = 0 \quad \text{at} \quad \rho = \rho_0, \\ \bar{w} = w/w_0, \quad P = \partial p/\partial z = \text{const.}, \quad w_0 = (-r_0^2P)/(4\mu), \\ \bar{\nabla}^2\bar{T}_2 = (a^2C^*w)/(\alpha T_w), \quad C^* = \partial T_2/\partial z = \text{const.}\end{gathered} \tag{20}$$

in which w and w_0 are respectively the velocities of the fluid at any point and at the center of the cutout, $\partial p/\partial z$ is the axial rate of change of pressure, μ is the dynamic viscosity, and $\alpha = K_2/C_p\rho_2^*$ is the thermal diffusivity. It should be mentioned that in this case the temperature of region 1 is also assumed to vary linearly along the length of the rectangular bar as does the temperature of the fluid. Since the fluid properties are independent from temperature, the velocity field is rotationally symmetric. This situation, however, is not the case for the temperature distribution. Employing dimensionless polar coordinates $\rho = r/a$ and φ at the center of the cutout (Fig. 1), the solutions of equations (20) are written in the following forms:

$$\begin{aligned}\bar{w} &= [1-\rho^2(a/r_0)^2], \\ \bar{T}_2 &= (\bar{T}_{p2})_1 + \sum_{n=0,1,2}^{\infty} \bar{A}_n\rho^n \cos(n\varphi) \\ &\quad + \sum_{n=1,2,3}^{\infty} \bar{B}_n\rho^n \sin(n\varphi), \\ (\bar{T}_{p2})_1 &= \lambda_1[\rho^2/4+(\rho^4/16)(a/r_0)^2], \\ \lambda_1 &= (a^2C^*w_0)/(\alpha T_w).\end{aligned} \tag{21}$$

Utilizing (21) in the definition of bulk temperature

$$\bar{T}_{\text{bulk}} = \frac{T_{\text{bulk}}}{T_w} - 1 = \frac{\int_0^{2\pi}\int_0^{r_0/a} [1-\rho^2(a/r_0)^2]\bar{T}_2\rho \, d\rho \, d\varphi}{\int_0^{2\pi}\int_0^{r_0/a} [1-\rho^2(a/r_0)^2]\rho \, d\rho \, d\varphi} \tag{22}$$

it is found that

$$\bar{T}_{\text{bulk}} = (8/3)\frac{\bar{A}_0}{(r_0/a)} + (5/42)\lambda_1(r_0/a). \tag{23}$$

Employing now the balance of the heat equation

$$\rho_2^*C_pC^*w_0\pi r_0^2 = -2\pi r_0 h_{\text{ave}}(T_{\text{bulk}} - T_w), \tag{24}$$

and defining a Nusselt number $(Nu)_{r_0}$ on the basis of the radius of the cutout r_0, the following result is obtained:

$$(Nu)_{r_0} = \frac{r_0 h_{\text{ave}}}{k_2} = -(\lambda_1/4)\frac{(r_0/a)^2}{\bar{T}_{\text{bulk}}}. \tag{25}$$

For case (2) of a uniformly distributed heat source per unit volume, $\dot{q}$, the equation for temperature is given by

$$\begin{gathered}\bar{\nabla}^2\bar{T}_2 = -\lambda_2, \\ \lambda_2 = -\frac{\dot{q}a^2}{k_2T_w}.\end{gathered} \tag{26}$$

The complementary solution for equation (26) has the same form as that given in equation (21), and its particular solution is

$$(\bar{T}_{p2})_2 = -(1/4)\lambda_2\rho^2. \tag{27}$$

It remains to satisfy the inner boundary conditions and determine the unknown constants of integration A_l, B_l and $\bar{A}_n$, $\bar{B}_n$ given in equations (17) and (21). In order to accomplish this goal for cases (1) and (2), p_1 and p_2 terms are respectively chosen in the series solutions given for $\bar{T}_1$ and $\bar{T}_2$. The boundary conditions (18) are then satisfied at M points in such a way that $2M > (p_1+p_2)$ giving a set of $2M$ linear equations with (p_1+p_2) unknowns. These equations are normalized and approximately solved by the technique of least square error [6]. For case (3), p terms in the series solution $\bar{T}_1$ are selected and the boundary condition(s) are satisfied at $M > p$ points of the inner boundary(ies) in one quadrant.

Table 1. The values of dimensionless temperature $\bar{T}_1 = \bar{T}_2$ at $\rho = \rho_0$ for case (1) with $\bar{c} = 0.25$, $\bar{d} = 0.125$, $\rho_0 = 0.0625$, $K = 0.07$, $\lambda_1 = 1000$, $N = 1$

	$\bar{T}_{\text{bulk}}$					
$(24/\pi)\phi_{\text{rad.}}$	1	3	5	7	9	11
$\bar{T}_1$	−0.07664	−0.07052	−0.06766	−0.06890	−0.07447	−0.08386
$(24/\pi)\phi_{\text{rad.}}$	13	15	17	19	21	23
$\bar{T}_1$	−0.09602	−0.1097	−0.1238	−0.1374	−0.1496	−0.1601
$(24/\pi)\phi_{\text{rad.}}$	25	27	29	31	33	35
$\bar{T}_1$	−0.1681	−0.1730	−0.1739	−0.1704	−0.1629	−0.1525
$(24/\pi)\phi_{\text{rad.}}$	37	39	41	43	45	47
$\bar{T}_1$	−0.1405	−0.1283	−0.1164	−0.1052	−0.09462	−0.08496

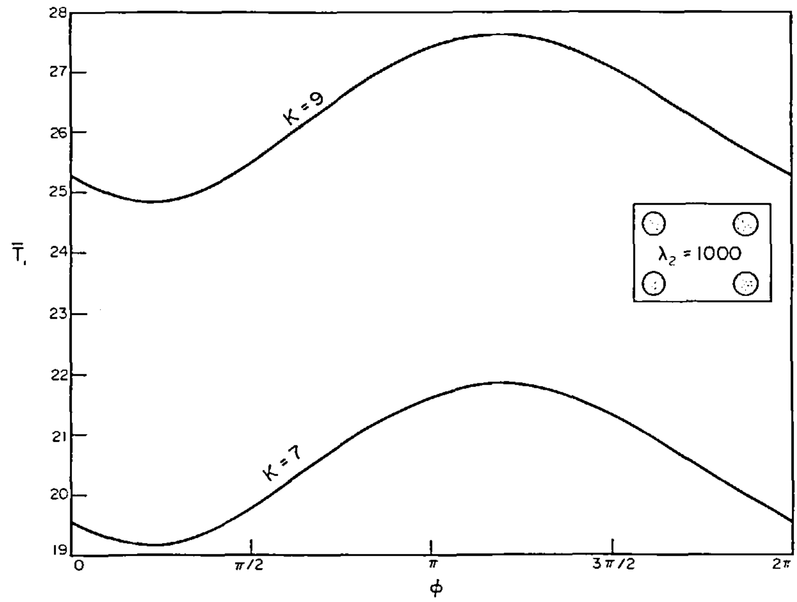

FIG. 2. The values of the dimensionless temperature around the boundary of two different materials in one quadrant.

From the fact that $\bar{A}_0$ depends on the ratio $K = k_1/k_2$, and that it is proportional to λ_1, it is seen from equations (23) and (25) that the Nusselt number is a function of geometry and properties of the two materials. The numerical examples presented here are on the basis of material properties in real situations. All of the numerical results with the exception of those for case (3) are for rectangular bars with four cutouts.

In Table 1, the values of dimensionless temperature $\bar{T}$ around the boundary of the two materials and $\bar{T}_{\text{bulk}}$ are presented for case (1) with $\lambda_1 = 1000$, and $K = 0.03$. In Table 2, the values of $(Nu)_{r_0}$ vs K are given for the fixed geometry of $\bar{C} = 0.25$, $\bar{d} = 0.125$, and $\bar{\rho}_0 = 0.0625$. In Fig. 2, the values of the dimensionless temperature around the boundary of two different materials with $K = 7$ and $K = 9$ are plotted for the case of uniformly distributed heat sources in the inner circles with $\lambda_2 = 1000$. In Fig. 3, the values of nondimensional conduction shape factors

$$\bar{S} = \frac{Q}{k_1(T_i - T_w)} \tag{28}$$

for a case of a rectangular bar with 8 circular cavities are plotted vs ρ_0 for $b/a = 0.5$ and $b/a = 0.6$. The dimensionless coordinates of the centers of the circular holes for this case are denoted by $\bar{c}_1, \bar{d}_1, \bar{c}_2$ and $\bar{d}_2$. For this case it is also assumed that the temperature T_i is the same for all 8 circular cavities.

Table 2. The values of Nusselt number $(Nu)_{r_0}$ vs K for case (1) with $\bar{c} = 0.25$, $\bar{d} = 0.125$, $\rho_0 = 0.0625$, and $N = 1$

K	0.03	0.05	0.07	0.09
$(Nu)_{r_0}$	0.03752	0.03552	0.03374	0.03213

CONCLUSION

For all of the numerical results presented in this investigation, the number of terms in the series solution and the number of points on the inner boundary(ies) in one quadrant are chosen in such a way that a system of

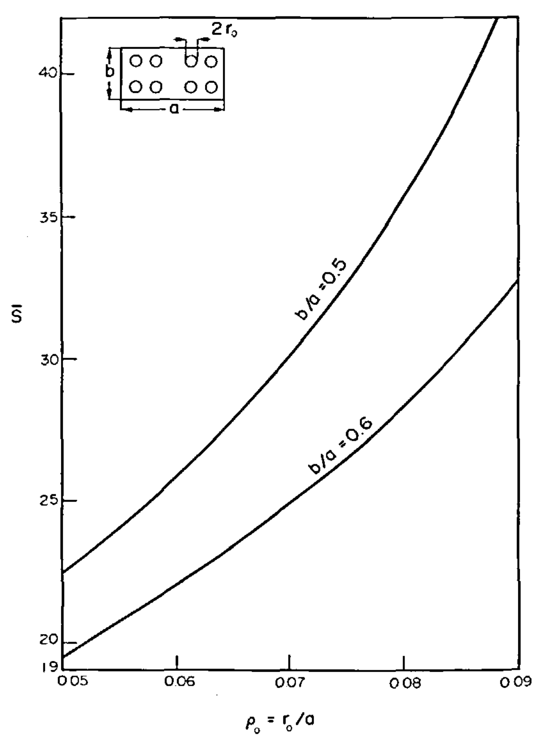

FIG. 3. The values of nondimensional shape factor $\bar{S}$ vs ρ_0 for two b/a ratios.

60 × 48 linear algebraic equations are obtained. The results found from the approximate solution of these equations [6] are very accurate and well within the usual engineering approximations. For example, in the case of a rectangular bar with 8 circular cavities, the relative error in satisfaction of the inner boundary condition $\bar{T}_1 = 1$ is of the order of 10^{-5} or less at the selected points.

When the material properties are assumed to be independent of temperature, the derived eigenfunctions produce a powerful technique for solving the steady state heat transfer problems in multiply-connected rectangular regions.

The method of solution can be extended to the case of a rectangular bar with noncircular cavities. It is also believed that similar eigenfunctions may be derived for the solutions of other applied mechanics problems such as three dimensional heat conduction in a rectangular parallelopiped with cylindrical cavities, and certain plate problems.

Acknowledgements—The author wishes to thank the Department of Computing Services of IUPUI for providing CDC 6600 computer time for this investigation.

REFERENCES

1. E. M. Sparrow and A. L. Loeffler, Jr, Longitudinal laminar flow between cylinders arranged in regular array, *A.I.Ch.E. Jl* 5, 325–330 (1959).
2. E. M. Sparrow, A. L. Leoffler, Jr and H. A. Hubbard, Heat transfer to longitudinal laminar flow between cylinders, *J. Heat Transfer* 83, 415–422 (1961).
3. J. C. Rowley and J. B. Payne, Steady state temperature solution for a heat generating circular cylinder cooled by a ring of holes, *Trans. Am. Soc. Mech. Engrs*, Series C, *J. Heat Transfer* 86, 531–536 (1964).
4. R. C. J. Howland, Potential functions periodicity in one coordinate, *Proc. Cambr. Phil. Soc.* 30, 315–326 (1935).
5. A. K. Naghdi, Solution of Poisson's equation in a rectangular region with multiple holes, *Proc. 10th South Eastern Conf. on Theoretical and Applied Mech.*, 10, 151–161 (1980).
6. F. B. Hildebrand, *Introduction to Numerical Analysis*. McGraw-Hill, New York (1956).

CERTAINS PROBLEMES THERMIQUES DANS UN DOMAINE RECTANGULAIRE AVEC PLUSIEURS FENETRES

Résumé—En employant un nouvelle famille de fonctions obtenue par amélioration d'une technique antérieure, on résoud les problèmes thermiques permanents suivants. (1) Une barre prismatique à base rectangulaire est refroidie ou chauffée par un fluide s'écoulant dans les bases circulaires de la barre. (2) Le transfert thermique dans une région rectangulaire qui a des sources thermiques uniformément distribuées avec différentes conductivités. (3) Conduction thermique dans une barre rectangulaire à plusieurs trous qui a différentes températures aux frontières d'entrée et de sortie. On suppose que les propriétés des matériaux sont indépendantes de la température. On présente des résultats numériques pour les cas des régions rectangulaires avec 4 et 8 cavités.

EINIGE WÄRMEÜBERTRAGUNGSPROBLEME IN EINEM RECHTECKIGEN GEBIET MIT MEHRFACHEN AUSSCHNITTEN

Zusammenfassung—Durch Anwendung einer neuen Klasse von Funktionen, welche durch Weiterentwicklung einer früheren Methode gewonnen wurden, konnten die folgenden stationären Wärmeübertragungsprobleme gelöst werden.

(1) Eine prismatischer rechteckiger Stab wird über ein Fluid das in kreisförmigen Ausschnitten des Stabes strömt, gekühlt oder beheizt.

(2) Wärmeübertragung in einem rechteckigen Gebiet mit gleichförmig verteilten Wärmequellen in kreisförmigen Einsätzen von unterschiedlicher Wärmeleitfähigkeit.

(3) Wärmeleitung in einem rechteckigen Stab mit mehreren Bohrungen und unterschiedlichen inneren und äußeren Wandtemperaturen.

Die Eigenschaften der Materialien wurden als temperaturunabhängig angenommen. Numerische Lösungen für rechteckige Gebiete mit 4 und 8 Hohlräumen werden angegeben.

НЕКОТОРЫЕ ЗАДАЧИ ТЕПЛОПЕРЕНОСА В ПРЯМОУГОЛЬНОЙ ОБЛАСТИ С МНОГОЧИСЛЕННЫМИ ПРОРЕЗЯМИ

Аннотация—С помощью нового класса функций, полученных после усовершенствования ранее развитого метода, решены следующие задачи стационарного теплопереноса: 1) призматический прямоугольный брусок охлаждается или нагревается потоком жидкости, проходящим через круглые отверстия в бруске; 2) теплоперенос в прямоугольной области с равномерно распределенными источниками тепла в круглых вставках с различной теплопроводностью; 3) передача тепла теплопроводностью в прямоугольном бруске с многочисленными отверстиями при разности температур на внутренней и внешней границах. Предполагается, что свойства используемых материалов не зависят от температуры. Представлены численные результаты для прямоугольных областей с 4 и 8 полостями.